

Implementing Gradient Model for Surface Roughness in WIPL-D

Milan P. Radović, Aleksandar Z. Golubović *Student Member, IEEE* and Miloš M. Jovičić

Abstract—The implementation of gradient method for surface roughness correction in WIPL-D software package is presented. Surface roughness model is tested on modified ring resonator model. Finally, simulation results from WIPL-D and CST Studio Suite are compared.

Index Terms—surface roughness, gradient model, effective conductivity, WIPL-D, ring resonator, surface impedance

I. INTRODUCTION

MODERN automotive radar systems are often developed in mm-Wave technology [1],[2] and require precise design and manufacturing. Hence, accurate full-wave electromagnetic modeling of such systems has an immense importance in development. To that aim, many electromagnetic effects, that are negligible at lower frequencies, should be taken into consideration at higher frequencies. One of such effects is surface roughness of conductors.

In this case study, gradient method [3] for surface roughness approximation is implemented in WIPL-D software package [4]. The implementation is tested on a model of modified ring resonator [5]. The results are then compared to the results acquired by CST Studio Suite [6].

Skin effect is a tendency of alternating currents to concentrate on the surfaces of conductors, and exponentially drop with conductor depth. It is a result of opposing Eddy currents induced by the changing magnetic fields. If a cylindrical wire-like conductor is observed, the countering Eddy currents will be strongest along the center of the cylinder and drop towards the surface. This will create a characteristic current density profile in the conductor, as shown in Fig. 1. With higher frequencies, currents are more concentrated at the surface of the conductor. We define skin depth, δ , as the depth at which the current density drops to $\frac{1}{e}$ of its value (around 36.7%)

Skin depth is given by [7]

$$\delta = \sqrt{\frac{2\rho}{\omega\mu}} \sqrt{\sqrt{1 + (\rho\omega\varepsilon)^2} + \rho\omega\varepsilon}, \quad (1)$$

Milan P. Radović is with the School of Electrical Engineering, University of Belgrade, 73 Bulevar kralja Aleksandra, 11020 Belgrade, Serbia and with NOVELIC d.o.o., Veljka Dugosevica 54/B5, 11000 Belgrade, Serbia (e-mail: milan.radovic@novelic.com).

Aleksandar Z. Golubović is with the School of Electrical Engineering, University of Belgrade and with NOVELIC d.o.o. (e-mail: aleksandar.golubovic@novelic.com).

Miloš M. Jovičić is with NOVELIC d.o.o. (e-mail: milos.jovicic@novelic.com)

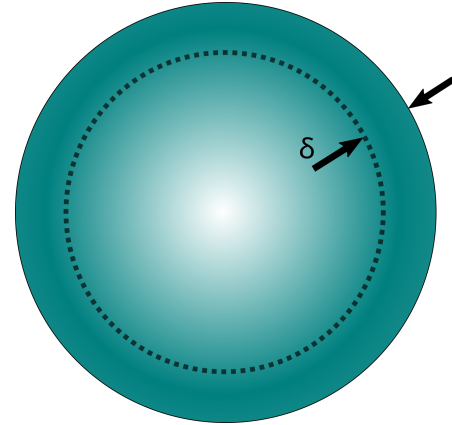


Fig. 1: Illustration of current density and the skin depth.

where ρ is the specific electrical resistance, ω is the angular frequency of current, μ is the permeability of the conductor and ε permittivity. At frequencies of interest, (1) can be approximated by

$$\delta = \sqrt{\frac{2}{\sigma\omega\mu}}. \quad (2)$$

At low frequencies, the skin depth is larger than the imperfections of the conductor surface. Therefore, when modeling conductors for electromagnetic analysis it is common to approximate the surface of the conductor as ideally flat. However, at high frequencies the skin depth is small enough that it is of comparable size to the roughness of the surface ($0.23 \mu\text{m}$ at 80 GHz). The rough surface of the conductor and the comparable skin depth qualitatively make the current paths longer. At microscopic levels, the roughness structures are electrically larger causing resonant frequencies to shift lower. Additionally, longer current paths will induce larger resistive losses.

We define R_q as the root mean square average of the profile height deviations from the mean line of ideal surface. Different copper deposition methods will yield different surface profiles with different R_q . Some of the most widely used copper profiles are [8] STD (Standard foil, $R_q = 5 - 10 \mu\text{m}$), HPF (High Performance Foil, $R_q = 10 - 15 \mu\text{m}$), RTF (Reverse Treated Foil, $R_q = 3 - 6 \mu\text{m}$), VLP (Very Low Profile, $R_q = 3 - 6 \mu\text{m}$), HVLP (Hyper Very Low Profile, $R_q = 1 - 3 \mu\text{m}$) and ULP (Ultra Low Profile, $R_q = 0.5 - 1 \mu\text{m}$), which are shown in Fig. 2. At 1 GHz , the skin depth is $2 \mu\text{m}$ and is considerably smaller than most copper profile R_q . Since

most of the high frequency current will be conducted through irregular boundary surface, it is important to realistically model and correct for the effects which the rough surface will induce.

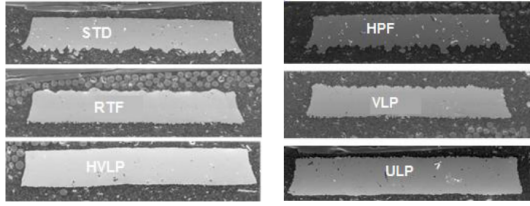


Fig. 2: Microscopic images of common copper deposition profiles.

II. GRADIENT METHOD

The gradient method relies on the fact that the surface profile can be described as a conductivity gradient, from conducting copper to non-conductive dielectric.

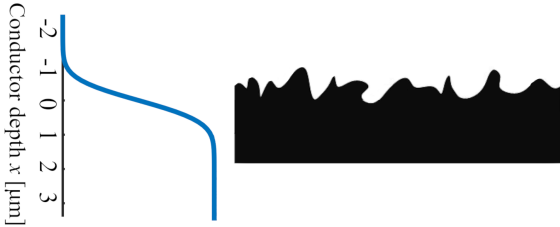


Fig. 3: An example of conductor surface profile and its cumulative distribution function.

It is evident from [3] that the conductivity, $\sigma(x)$, is a cumulative distribution function of x

$$\sigma(x) \propto CDF(x). \quad (3)$$

Cumulative distribution function is given as the integral of probability distribution function over the entire x domain

$$CDF(x) = \int_{-\infty}^x PDF(u)du. \quad (4)$$

We approximate the probability distribution function with a normal Gauss distribution

$$PDF(x) = \frac{1}{R_q\sqrt{2\pi}} e^{-\frac{x^2}{2R_q^2}}. \quad (5)$$

Finally, the conductivity function can be written as

$$\sigma = \sigma_0 CDF(x) = \sigma_0 \int_{-\infty}^x \frac{1}{R_q\sqrt{2\pi}} e^{-\frac{u^2}{2R_q^2}} du. \quad (6)$$

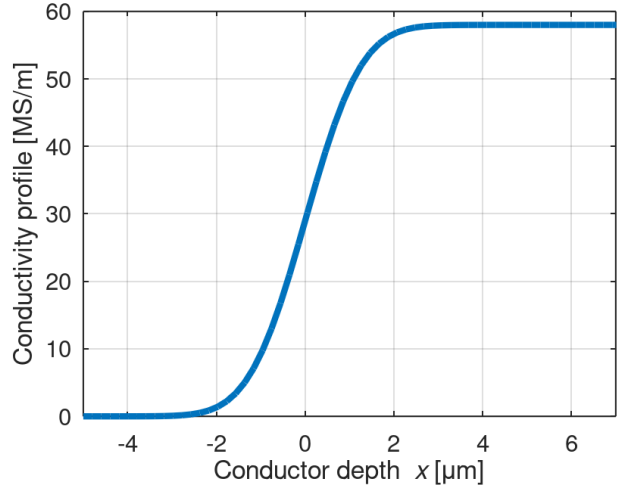


Fig. 4: Conductivity profile of copper surface for $R_q = 1 \mu\text{m}$.

Next, wave equations are derived with additional term that corresponds to variable conductivity due to surface roughness [3]

$$\frac{\partial^2 B_y}{\partial x^2} - j\omega\mu_0\sigma B_y - \frac{\partial}{\partial x} \ln(\sigma(x)) \frac{\partial B_y}{\partial x} = 0, \quad (7)$$

where B is magnetic flux density vector. It should be noted that when the conductivity profile is constant, (7) simplifies down to classical Helmholtz equation which is analytically solvable. However, (7) needs to be numerically solved.

Finite differences method is used to solve (7) for B_y . The results are presented in Fig. 5.

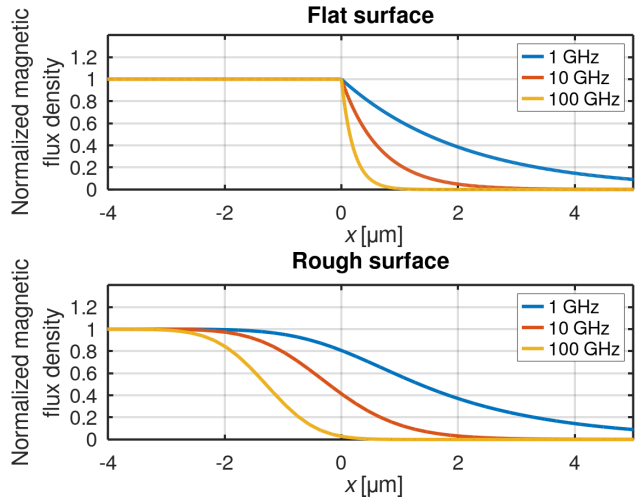


Fig. 5: Comparison of magnetic flux density y component for flat and rough surface ($R_q = 1 \mu\text{m}$).

The change in magnetic flux density is gradual and not sharp as in the flat approximation, which is more in accordance to the real scenario. Knowing the magnetic flux density it is possible to find the current density distribution given by Fig. 6

$$J_z = \frac{1}{\mu_0} \frac{\partial B_y}{\partial x}. \quad (8)$$

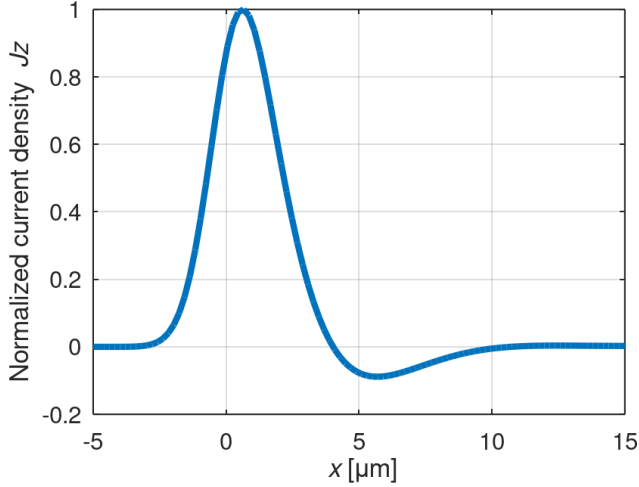


Fig. 6: Normalized current density distribution.

III. EFFECTIVE CONDUCTIVITY

The power density of the conductor surface is given by [3]

$$P_d = \int_{\sigma>0} \frac{|J|^2}{2\sigma(x)} dx. \quad (9)$$

Consider another conductor with a flat surface that has the same power density as observed rough surface conductor. Its conductivity profile will be a step function

$$\sigma(x) = \begin{cases} \sigma_{\text{eff}}, & x < 0 \\ 0, & x > 0 \end{cases}. \quad (10)$$

By equalizing the two power distributions, we can calculate the effective conductivity that a flat conductor will need to have, in order to reproduce the same power distribution as a rough surfaced one

$$\int_{\sigma>0} \frac{|J_{\text{rough}}|^2}{2\sigma(x)} dx = \int_{\sigma>0} \frac{|J_{\text{flat}}|^2}{2\sigma_{\text{eff}}} dx. \quad (11)$$

Finally, effective conductivity for different R_q values is numerically computed (7).

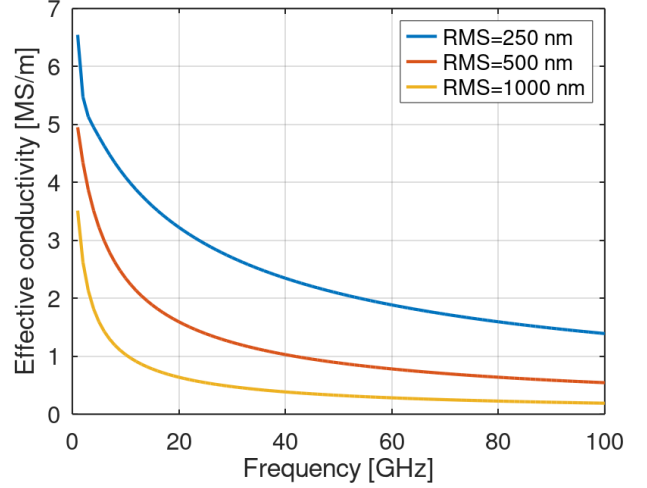


Fig. 7: Comparison of effective conductivity in function of frequency for different values of R_q .

IV. EFFECTIVE PERMEABILITY

Previous method models the resistive losses that will be induced from the surface roughness, however, due to different surface profile the conductor will have different reactive losses.

Similarly to previous modeling of effective conductivity, we will model an effective permeability to account for reactive losses. We observe another conductor with identical magnetic field energy distribution, however, with effective permeability. Equalizing the two energy distributions we can calculate the effective permeability as

$$\int_{\sigma>0} \frac{|B_{y,\text{rough}}|^2}{2\mu_0\mu_r} dx = \int_{\sigma>0} \frac{|B_{y,\text{flat}}|^2}{2\mu_0\mu_{r,\text{eff}}} dx. \quad (12)$$

By numerically solving, we yield (Fig. 8):

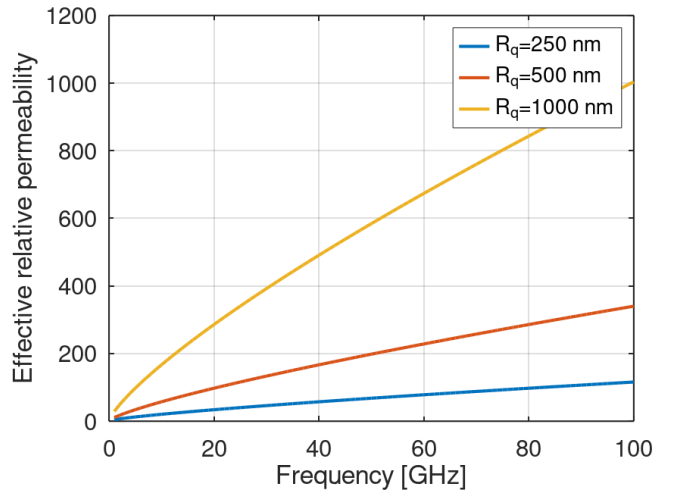


Fig. 8: Comparison of effective permeability in function of frequency for different values of R_q .

V. IMPLEMENTATION AND RESULTS

By obtaining both conductivity and permeability, we can model both resistive and reactive losses. The software package WIPL-D can model distributed loadings with surface impedance, hence we need to translate our parameters into surface impedance as,

$$Z_s = R_s + jX_s = \frac{1}{\sigma_{\text{eff}}\delta(\sigma_{\text{eff}})} + \frac{1}{\sigma_0\delta(\mu_{r,\text{eff}})}. \quad (13)$$

We model a modified ring resonator in both WIPL-D and CST Studio Suite for the purposes of result comparison (Figure 9). In CST we use the surface roughness method provided with the software, while in WIPL-D we use the frequency table function to implement the surface impedance into the model.

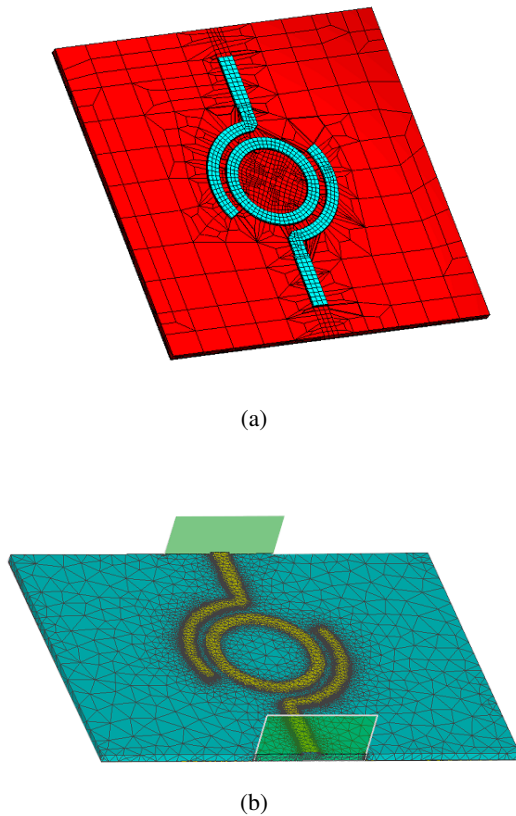


Fig. 9: a) Ring resonator model in WIPL-D and b) ring resonator model in CST

Since CST uses gradient method that accurately model surface roughness, matching of results obtained by CST and WIPL-D will prove a successful implementation of gradient method in WIPL-D.

The comparison of simulated reflection coefficient for both flat and rough surface of modified ring resonator is shown in 10. From these figures we can observe that there is an excellent matching between the results, thus the gradient method is successfully implemented in WIPL-D.

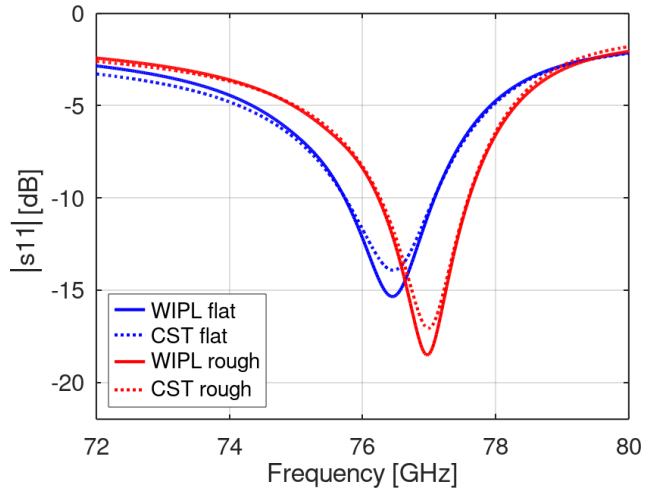


Fig. 10: Comparison of s_{11} for CST and WIPL-D.

VI. CONCLUSION

Gradient method for surface roughness estimation is implemented in WIPL-D and tested on modified ring resonator model. Results match the ones obtained using CST Studio Suite, thus gradient model implementation is corroborated. This method can be utilized in WIPL-D, for mm-Wave designs, where surface roughness is crucial.

REFERENCES

- [1] Baolong Jian, Jing Yuan, and Qiqin Liu. "Procedure to Design a Series-fed Microstrip Patch Antenna Array for 77 GHz Automotive Radar". In: *2019 Cross Strait Quad-Regional Radio Science and Wireless Technology Conference (CSQRWC)*. 2019, pp. 1–2.
- [2] Sungjun Yoo et al. "Patch Array Antenna Using a Dual Coupled Feeding Structure for 79 GHz Automotive Radar Applications". In: *IEEE Antennas and Wireless Propagation Letters* 19.4 (2020), pp. 676–679.
- [3] Gerald Gold and Klaus Helmreich. "A Physical Surface Roughness Model and Its Applications". In: *IEEE Transactions on Microwave Theory and Techniques* 65.10 (2017), pp. 3720–3732.
- [4] WIPL-D. <https://wipl-d.com>.
- [5] Piotr Jankowski-Miñulowicz et al. "Determination of the Material Relative Permittivity in the UHF Band by Using T and Modified Ring Resonators". In: *International Journal of Electronics and Telecommunications* 62 (June 2016).
- [6] CST Studio Suite. <https://www.3ds.com/products-services/simulia/products/cst-studio-suite>.
- [7] Vander Vorst Andre; Rosen Arye; Kotsuka Youji. *RF/Microwave Interaction with Biological Tissues*. Wiley-Interscience, p. 41.
- [8] Aleksei V. Rakov et al. "Quantification of Conductor Surface Roughness Profiles in Printed Circuit Boards". In: *IEEE Transactions on Electromagnetic Compatibility* 57.2 (2015), pp. 264–273.